New description of stress-induced anisotropy using modified stress

Une nouvelle description de l'anisotropie induite par les contraintes utilisant la contraintes modifiée

M. Kikumoto, T. Nakai and H. Kyokawa
Nagoya Institute of Technology, Nagoya, Japan

ABSTRACT

A simple and comprehensive method for describing the influences of the intermediate principal stress σ_2 and the stress histories on the deformation and the strength of soils, which assumes associated flow rule and obeys isotropic hardening rule in modified stress space, is proposed. The concept of the modified stress t_{ij}, which was proposed to describe the influence of σ_2, is extended to the proposed modified stress tensor t_{ij}^* to consider the fabric change of soils due to the stress histories as well as the variation of σ_2. In this paper, the modified stress t_{ij}^* is applied to an elastoplastic model named subloading t_{ij} model. The proposed model is verified by comparing the calculated results with the experimental results on sand.

RÉSUMÉ

Une méthode simple est proposée pour la description de l'influence de la contrainte principale intermédiaire et de l'histoire du chargement sur la déformation et la résistance des sols. Cette méthode considère le flux associé et obéit à la loi de durcissement isotropique dans l'espace des contraintes modifiées. Le concept de contrainte modifiée t_{ij}, proposé pour décrire l'influence de la contrainte principale intermédiaire, est étendu au tenseur de contraintes modifiées t_{ij}^* pour tenir compte du changement de structure des sols relatif à la fois l'histoire du chargement et à la variation de la contrainte principale intermédiaire. Dans ce papier, la contrainte modifiée t_{ij}^* est appliquée à un modèle élasto-plastique appelé modèle à sous-chargement t_{ij}. Le modèle proposé est vérifié en comparant les résultats de calcul à des résultats expérimentaux sur sable.

Keywords : elastoplastic model, induced anisotropy, isotropic hardening rule, associated flow, modified stress

1 INTRODUCTION

It is usually mentioned that the intermediate principal stress σ_2 and the stress histories have large influences on the deformation and the strength of soil. It has, however, been considered that the influence of σ_2 and the influence of stress path are different features. In the ordinary models, the influence of σ_2 is usually considered by assuming a non-circular shaped yield surface in octahedral plane (or by changing the strength depending on the relative magnitude of σ_2). The influence of the stress histories is considered by applying kinematic / rotational hardening rule in ordinary stress space. The authors have proposed the concept of the modified stress t_{ij} and developed an isotropic hardening model based on this concept, which can take into consideration of the influence of σ_2 automatically. Here, t_{ij} is a modified stress tensor reflecting the fabric change due to monotonous shear loading – i.e., stress-induced anisotropy.

A new method, in which the induced anisotropy of soil is described by applying modified stress in stead of ordinary stress, is developed in this study. The proposed method obeys simple and general isotropic hardening rule in the modified stress space. In addition, the proposed method is an extension of the concept of t_{ij}, and hence it can simultaneously evaluate the influence of σ_2. In this paper, the outline of the proposed method is presented and the method is verified by the results of true triaxial tests and directional shear cell tests on sand.

2 MODIFIED STRESS t_{ij} AND ITS RELATION WITH STRESS-INDUCED ANISOTROPY OF SOILS

2.1 *The outline of the concept of the modified stress t_{ij}*

In most of isotropic hardening models such as Cam clay model, their yield functions are formulated using parameters of ordinary stress σ_{ij} and the flow rule is assumed in σ_{ij}-space. Such models, however, cannot describe the strength and the deformation of soils in three-dimensional stresses in a uniform manner. Nakai & Mihara (1984) proposed a method, in which the yield function is formulated using the parameters of the modified stress t_{ij} and the flow rule is assumed in t_{ij}-space. This method can suitably consider the influence of σ_2 by the parameters of stress and strain increment based on spacially mobilized plane (Matsuoka & Nakai 1974) listed in Table 1. The key points are: (i) the transform tensor a_{ij} for obtaining t_{ij} is coaxial with σ_{ij}. (ii) the ratio of principal values of a_{ij} is proportional to that of principal stresses to the minus one half.

Table 1. Comparison of stress and strain increment parameters in ordinary, t_{ij} and t_{ij}^* concept.

ordinary concept	t_{ij} concept	t_{ij}^* concept
δ_{ij}	$a_{ij}=\sqrt{I_3/I_2}\,r_{ij}^{-1}$ $\left(r_{ik}r_{kj}=\sigma_{ij}\right)$	a_{ij}^* $a_{ij}^\#$
σ_{ij}	$t_{ij}=a_{ik}\sigma_{kj}$	$t_{ij}^*=(a_{ik}^*\sigma_{kj}+\sigma_{ik}a_{kj}^*)/2$
$p=\sigma_{ij}\delta_{ij}/3$	$t_N=t_{ij}a_{ij}$	$t_N^*=t_{ij}^*a_{ij}^\#$
$s_{ij}=\sigma_{ij}-p\delta_{ij}$	$t'_{ij}=t_{ij}-t_Na_{ij}$	$t'^*_{ij}=t_{ij}^*-t_N^*\,a_{ij}^\#$
$q=\sqrt{(3/2)s_{ij}s_{ij}}$	$t_S=\sqrt{t'_{ij}t'_{ij}}$	$t_S^*=\sqrt{t'^*_{ij}t'^*_{ij}}$
$\eta_{ij}=s_{ij}/p$	$x_{ij}=t'_{ij}/t_N$	$x_{ij}^*=t'^*_{ij}/t_N^*$
$\eta=q/p=\sqrt{\eta_{ij}\eta_{ij}}$	$X=t_S/t_N=\sqrt{x_{ij}x_{ij}}$	$X^*=t_S^*/t_N^*=\sqrt{x_{ij}^*x_{ij}^*}$
$d\varepsilon_v=d\varepsilon_{ij}\delta_{ij}$	$d\varepsilon_N=d\varepsilon_{ij}a_{ij}$	$d\varepsilon_N^*=d\varepsilon_{ij}a_{ij}^\#$
$de_{ij}=d\varepsilon_{ij}-d\varepsilon_v\delta_{ij}/3$	$d\varepsilon'_{ij}=d\varepsilon_{ij}-d\varepsilon_Na_{ij}$	$d\varepsilon'^*_{ij}=d\varepsilon_{ij}-d\varepsilon_N^*a_{ij}^\#$
$d\varepsilon_d=\sqrt{(2/3)de_{ij}de_{ij}}$	$d\varepsilon_S=\sqrt{d\varepsilon'_{ij}d\varepsilon'_{ij}}$	$d\varepsilon_S^*=\sqrt{d\varepsilon'^*_{ij}d\varepsilon'^*_{ij}}$
$d\varepsilon_{ij}^p=\Lambda\dfrac{\partial f}{\partial\sigma_{ij}}$	$d\varepsilon_{ij}^p=\Lambda\dfrac{\partial f}{\partial t_{ij}}$	$d\varepsilon_{ij}^p=\Lambda\dfrac{\partial f}{\partial t_{ij}^*}$

Proceedings of the 17th International Conference on Soil Mechanics and Geotechnical Engineering
M. Hamza et al. (Eds.)

doi:10.3233/978-1-60750-031-5-550

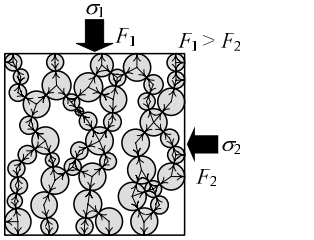

(a) Increase of the interparticle contact normals in σ_1 direction due to the increase of stress ratio

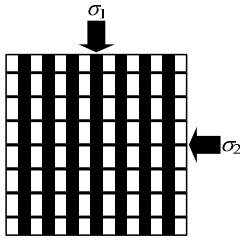

(b) Anisotropic continuum considering the concentration of contact normals

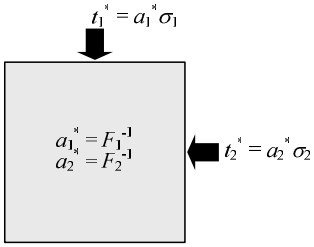

(c) Isotropic continuum equivalently transformed by modified stress

Figure 1. Modeling of induced anisotropy using modified stress.

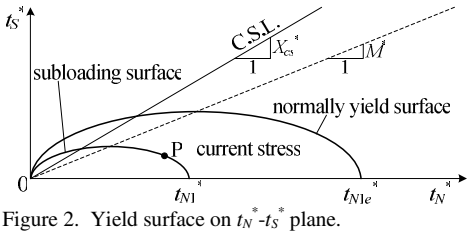

Figure 2. Yield surface on t_N^*-t_S^* plane.

2.2 *Description of the stress-induced anisotropy of soil by the modified stress*

It has been indicated based on microscopic observations by Oda (1972) that the distribution of the interparticle contact normals, which is represented by a second order fabric tensor F_{ij}, gradually tends to concentrate towards the direction of the major principal stress σ_1 when anisotropic stress acts on soil skeleton as shown in Fig. 1 (a). In continuum mechanics, this is equivalent to a relative increase of stiffness in σ_1-direction as indicated in Fig. 1 (b). By applying a modified stress whose stress ratio is smaller than σ_1/σ_2, such anisotropic behavior of granular material can be modeled as an isotropic material as shown in Fig. 1 (c). Thus, modified stress t_{ij}^* which is transformed by the fabric tensor F_{ij} reflecting the past stress histories is proposed to describe the induced anisotropy within a simple isotropic hardening model. It has been noticed by Satake (1982) that t_{ij}^* defined in Eq. (1), supposing that a_{ij}^{*-1} represents the fabric tensor F_{ij}, suitably consider the induced anisotropy.

$$t_{ij}^* = \frac{a_{ik}^* \sigma_{kj} + \sigma_{ik} a_{kj}^*}{2} \tag{1}$$

It has been indicated that the transform tensor a_{ij}^* is coaxial with σ_{ij} (Oda 1972) and the ratio of its principal values is proportional to that of principal stresses to the minus one half under monotonic loading paths (Satake 1982).

2.3 *Relation of the modified stress t_{ij} with induced anisotropy*

It is obvious from sections 2.1 and 2.2 that a_{ij} is equivalent to a_{ij}^* under monotonous loading paths. Therefore, a_{ij} (t_{ij}) can be regarded as a mechanical quantity considering the induced anisotropy under monotonic loading. In the present study, the modified stress t_{ij} is hence extended to a new stress tensor t_{ij}^* so that it can consider the fabric change due to the variation of σ_2 and the stress histories under general three-dimensional stress paths including rotation of principal stress axes.

3 MODIFIED STRESS t_{ij}^* CONSIDERING THE INFLUENCES OF σ_2 AND STRESS HISTORIES

In extending the modified stress t_{ij} to a new mechanical quantity t_{ij}^*, the evolution rule of the transformation tensor a_{ij}^* is determined satisfying the following experimental and numerical evidences (e.g. Satake 1982).

a) a_{ij}^* is equal to a_{ij} under monotonic loading paths without rotations of principal stress axes.
b) a_{ij}^* coincides with a_{ij} near / at failure even under complex stress paths because the strength of soils is independent of the stress histories.
c) a_{ij}^* is fixed during unloading as the soil fabric hardly changes during elastic deformation.
d) a_{ij}^* gradually approaches to a_{ij} with the development of plastic deformation although a_{ij}^* differs from a_{ij} under complex loading paths.

An example of evolution rules of a_{ij}^* which satisfies all of the above-mentioned requirements is given by Eq. (2).

$$\begin{aligned} da_{ij}^* &= k da_{ij} + l\left(a_{ij} - a_{ij}^*\right) \\ &= \left(\cos\frac{\theta}{2}\right) da_{ij} + \mu\sqrt{d\varepsilon_{kl}^p d\varepsilon_{kl}^p}\left(a_{ij} - a_{ij}^*\right) \end{aligned} \tag{2}$$

k represents loading directions, namely, monotonic loading (k = 1), non-monotonic loading ($0 < k < 1$) and unloading (k = 0). θ is given by the stress ratio tensor x_{ij}^* and its increment dx_{ij}^* as:

$$\theta = \cos^{-1}\left(\frac{x_{ij}^* dx_{ij}^*}{\sqrt{x_{kl}^* x_{kl}^*}\sqrt{dx_{mn}^* dx_{mn}^*}}\right) \tag{3}$$

l is proportional to the magnitude of plastic strain increment $d\varepsilon_{ij}^p$, while μ is a newly added parameter representing the rate of the decay of the influence of stress histories.

In the concept of t_{ij}, a_{ij} is applied not only for converting σ_{ij} into t_{ij} but also for dividing t_{ij} and $d\varepsilon_{ij}^p$ into their parameters. In the present method, a_{ij}^* is, however, non-coaxial with t_{ij}^*. Thus, in order to formulate an isotropic hardening model, a unit tensor $a_{ij}^\#$ coaxial with t_{ij}^* is newly employed for dividing t_{ij}^* and $d\varepsilon_{ij}^p$ into their parameters. In consideration of the relation between t_{ij} and a_{ij}, $a_{ij}^\#$ can be expressed by t_{ij}^* in the same form as a_{ij}.

4 APPLICATION OF THE MODIFIED STRESS t_{ij}^* TO AN ISOTROPIC HARDENING ELASTOPLSTIC MODEL

The proposed concept of the modified stress t_{ij}^* can be applied to any isotropic hardening model. In this paper, an elastoplastic model named subloading t_{ij} model is extended by t_{ij}^* to take into account of the induced anisotropy. Since the details of the original model are explained in other paper (Nakai & Hinokio 2004), application of t_{ij}^* to the subloading t_{ij} model is mainly presented here. The method of applying t_{ij}^* is quite simple, viz., defining the yield function f by the parameters of t_{ij}^* as eq. (4) and assuming associated flow rule in t_{ij}^*-space as eq. (5).

$$f = \ln t_N^* + \frac{1}{\beta}\left(\frac{X^*}{M^*}\right)^\beta - \ln t_{N1}^* = 0 \tag{4}$$

$$d\varepsilon_{ij}^p = \Lambda \frac{\partial f(t_{ij}^*, a_{ij}^\#)}{\partial t_{ij}^*} \tag{5}$$

Here, β is a material parameter determining the shape of the yield surface. The valuable t_{N1}^* is a hardening parameter determining the size of the yield surface, which is linked with the plastic volumetric strain as Cam clay model. The parameter M^* is a constant expressed using stress ratio X_{CS}^* and plastic strain increment ratio Y_{CS}^* at critical state. The proportional constant Λ is obtained by Prager's consistency equation (df = 0).

Figure 2 illustrates the yield surface on t_N^*-t_S^* plane.

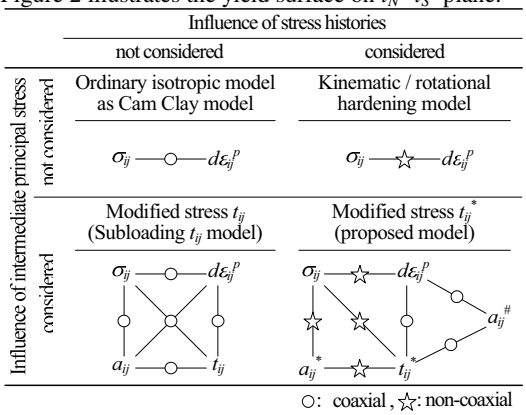

Figure 3. Comparison between the proposed model and other models.

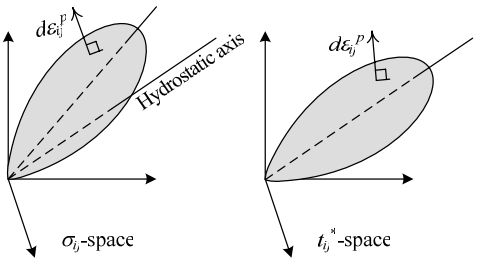

Figure 4. Comparison of the method for describing induced anisotropy.

The characteristics of the proposed model and other models are summarized in Figs. 3 and 4. The influence of σ_2 and that of the stress histories are described inclusively by a simple isotropic hardening model. In the proposed method, yield function with non-circular shaped section in octahedral plane and kinematic / rotational hardening rule are no more necessary for considering the induced anisotropy, that is, hardening parameters and constitutive parameters for such hardening rule are not required. In addition, the non-coaxiality between σ_{ij} and $d\varepsilon_{ij}^p$ can also be described by the proposed model even though it obeys isotropic hardening rule in the t_{ij}^* space.

5 EXPERIMENTAL VALIDATION OF THE PROPOSED METHOD

In this section, the concept of the modified stress t_{ij}^* is verified by comparing the calculated results with experiment results on medium dense Leighton Buzzard sand (e_{max} = 0.815, e_{min} = 0.516, G_s = 2.66, D_r = 72 %) conducted by Alawaji, et al. (1987). It is experimentally confirmed that the samples used in the tests have negligible initial stress anisotropy.

The material parameters in the proposed model are listed in Table 2. μ controls the rate of the decay of the influence of stress histories due to the development of the plastic strain. Other parameters are the same as those of the original model. These parameters are determined from the results of isotropic compression test and true triaxial test under constant Lode angle.

First, the results of true triaxial tests under constant mean principal stress are shown in Figs. 5 and 6. In these tests, each sample was firstly sheared in the radial direction on the octahedral plane from A ((σ_x, σ_y, σ_z) = (34.5, 34.5, 34.5) kPa) to C ((52.2, 15.9, 32.4) kPa), which is monotonic loading, and then unloaded to I ((41.4, 27.6, 34.5) kPa). Finally, the samples were sheared to the direction of 1, 4 and 7, respectively. Fig. 5 shows the relationships between stress ratio (q/p), principal strains (ε_x, ε_y and ε_z) and volumetric strain (ε_v), in which dots denote observed results, solid lines denote calculated ones by the proposed model, and broken lines denote calculated ones by subloading t_{ij} model. Fig. 6 shows the vectors of shear strain increment along various stress paths on octahedral plane. The length of each arrow which represents the directions of the shear strain increment is given by the shear strain increment divided by the increment of shear stress ratio on the octahedral plane.

Table 2. Constitutive parameters and its values.

λ		0.0320	
κ		0.0020	
e_{NC} at p = 98 kPa & q = 0 kPa		1.05	Same parameters as Cam clay model
$R_{cs} = (\sigma_1/\sigma_3)_{cs(comp.)}$		2.6	
ν_e		0.2	
β		1.6	Shape of yield surface (same as original Cam clay if β= 1)
a	a_{AF}	15	Influence of density and confining pressure
	a_{IC}	85	
μ		40	Influence of stress history

It is seen from these figures that the calculated results by the proposed model and the former model are identical from A to C, because newly proposed t_{ij}^* coincides with t_{ij} under monotonic loading paths. It can be said that the calculated results agree well with the test results in the probes A to C, that is, the stiffness decreases with the increasing of stress ratio q/p.

In the unloading region (probes C to I), both models properly describe the elastic behavior observed in the tests. In the proposed model, a_{ij}^* remains constant during unloading and the prediction by the model becomes different from that by subloading t_{ij} model after the stress state I.

During reloading from I to 1, it is seen that calculated results by subloading t_{ij} model underestimate the increase of shear stiffness as the soil is assumed to be elastoplastic in the reloading path due to the subloading surface. Meanwhile, the proposed model is able to describe precisely the increase of stiffness. Therefore, it is possible to say that t_{ij}^* suitably considers the influence of stress histories. The same results can be seen in the loading path ACI4. By comparing the shear strain increment in the stress path I to 4, subloading t_{ij} model does not completely coincide with the experimental results, which is caused by the fact that the direction of plastic strain increment is only determined by the present stress condition regardless of the stress histories in an ordinary isotropic hardening model. On the other hand, the proposed model agrees well with the experimental results both in direction and length of strain increment. Therefore, it can be concluded that a model using t_{ij}^* can properly consider the influence of the stress histories under complex stress paths, in spite of isotropic hardening model. In stress path ACI7, the proposed model can describe both the reduction of the stiffness and the dilatancy before reaching an isotropic stress state along path C-I-7, while subloading t_{ij} model exhibits only elastic deformation in this stress path.

The results of directional shear cell tests under plane strain condition (ε_z = 0) are shown in Figs. 7 and 8. The major and minor principal stresses in shearing plane (x:y plane) are constant in all the tests. The principal stress axes rotate 90 degrees under plane strain condition (ε_z = 0) from a stress state ((σ_x - σ_y) / 2 = 17.9 kPa, τ = 0 kPa) and then back to the original stress condition. Fig. 7 indicates the variation of each strain component with the angle between x-axis and major principal stress axis. In Fig. 8, the stress paths in the (σ_x - σ_y)/2:τ_{xy} plane are shown together with the directions of strain increments represented by the conjugate $d\gamma_{xy}$/2:($d\varepsilon_x$ - $d\varepsilon_y$)/2 relation.

It is seen from the experimental results that there seems no coaxiality between stresses and strain increments during the rotation of principal stress axes; the elastic region exists just after reversed rotation in the same way as reversed shear loading. The original model exhibits little strain during the rotation of the principal stress axes because stress invariants of ordinary isotropic hardening model remain constant under pure rotation of the principal stress axes. In contrast, there is rather good agreement between the observed results and the results calculated by the proposed model including the development of plastic strain due to the rotation of principal stress axes and non-coaxiality between stress and strain increment.

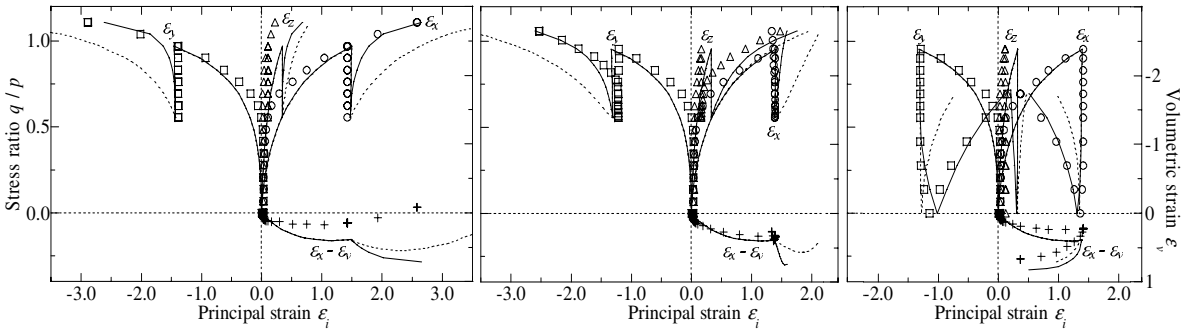

Figure 6. True triaxial tests: Stress-strain relations (Stress path ACI)

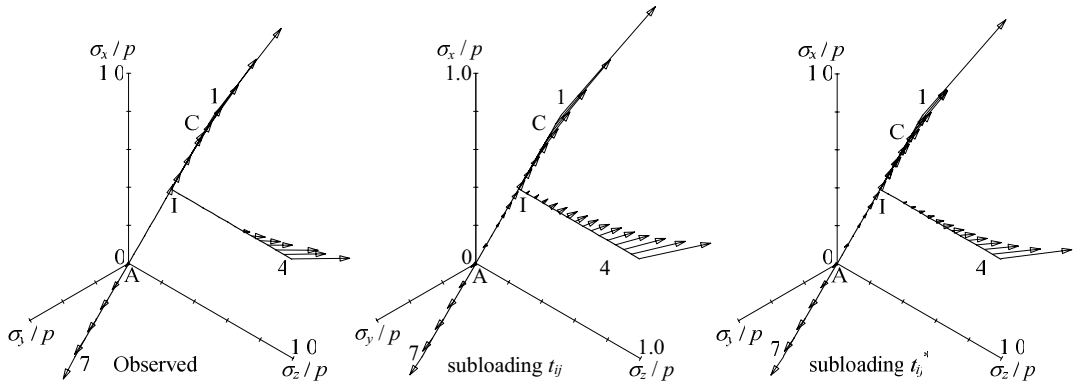

Figure 7. True triaxial tests: Stress paths and strain increment vectors (Stress paths ACI1, ACI4, ACI7)

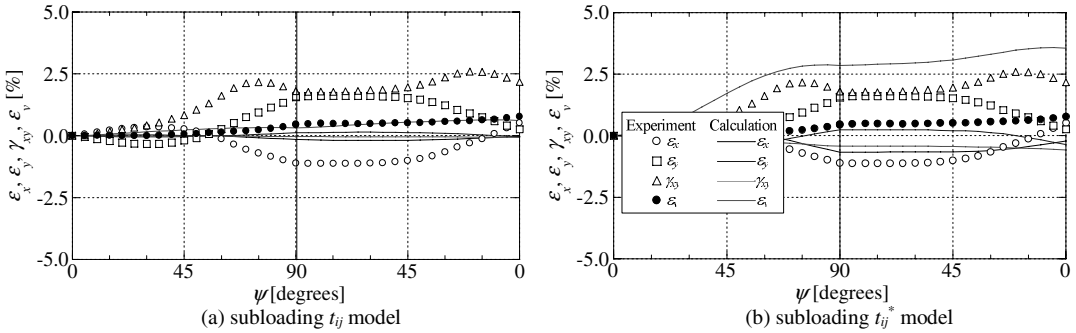

Figure 8. Directional shear cell test: Stress-strain relations of experiments and analysis (rotation of principal stress axes).

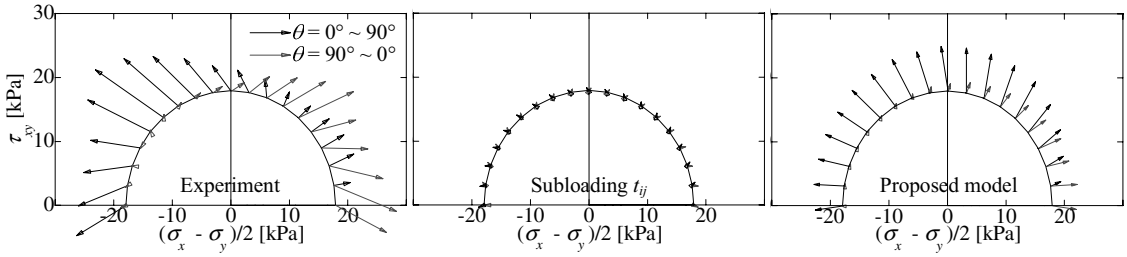

Figure 9. Directional shear cell test: Stress paths and strain increment vectors (rotation of principal stress axes).

6 CONCLUSIONS

The modified stress t_{ij}, which was proposed to consider the influence of intermediate principal stress σ_2, is extended to a new modified stress t_{ij}^*, so that it can describe the influences of σ_2 and stress histories all together, namely, the stress-induced anisotropy. The modified stress t_{ij}^* is, then, introduced to an isotropic hardening model named subloading t_{ij} model to extended to describe the induced anisotropy of soil as well.

The proposed subloading t_{ij}^* model is verified with the results of true triaxial tests and directional shear cell tests on sand. It is shown from two series of simulations that the proposed model, which obeys isotropic hardening rule and assumes associated flow rule in t_{ij}^*-space, properly reproduces the test results under various complex three-dimensional stress path including rotation of principal stress axes.

REFERENCES

Alawaji, M. M., Sture, S. & Ko, H. Y. 1987. True triaxial and directional shear cell experiments on dry sand, Interim technical report, University of Colorado.

Matsuoka, H. & Nakai, T. 1974. Stress-deformation and strength characteristics of soil under three different principal stresses, Proc. JSCE 232 : 59-70.

Nakai, T. & Hinokio, M. 2004. A simple elastoplastic model for normally and over consolidated soils with unified material parameters, S&F 44(2) : 53-70.

Nakai, T. & Mihara, Y. 1984. A new mechanical quantity for soils and its application to elastoplastic constitutive models, S&F 24(2) : 82-94.

Oda, M. 1972. The mechanism of fabric changes during compressional deformation of sand, S&F 12(2) : 1-18.

Satake, M. 1982. Fabric tensor in granular materials, Proc. of IUTAM-Conf. on Deformation and Failure of Granular Materials : 63-68.